NLO QCD CORRECTIONS TO INCLUSIVE J/ψ AND Υ PHOTOPRODUCTION CROSS SECTIONS FROM HERA TO THE EIC

Yelyzaveta Yedelkina

C. Flore, J.-Ph. Lansberg, H.-Sh. Shao, A. Colpani Serri, Yu Feng, M. A. Ozcelik, M. Nefedov

July 8, 2024

Synergies between LHC and EIC for quarkonium physics

General structure of NLO corrections

M. Krämer, Nucl.Phys., B459, 3 (96')

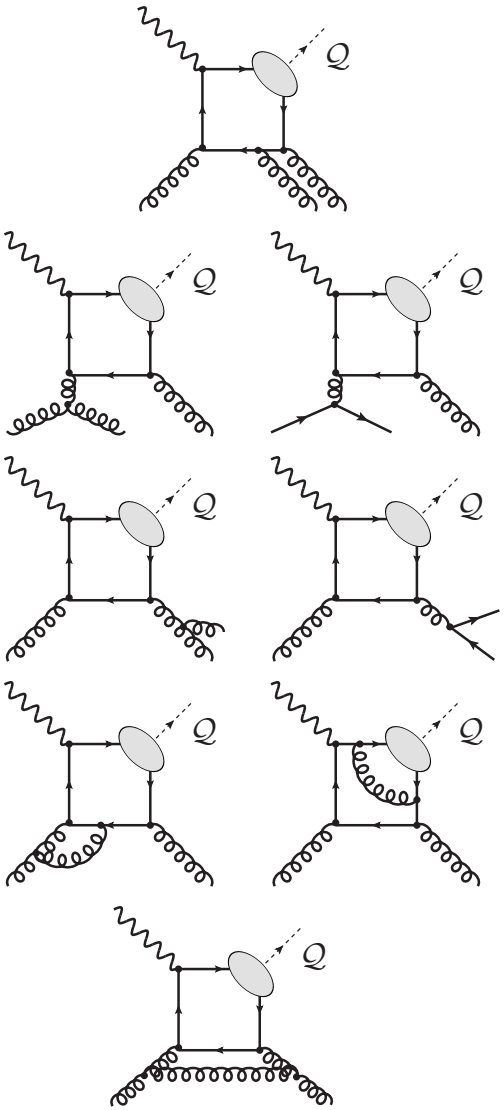

Singularities at NLO [and how they are removed]:

- Real emission
  - Infrared divergences: Soft [cancelled by loop IR contr.]
  - Infrared divergences: Collinear
    - ★ initial state [subtracted via "renormalisation" of collinear PDFs (Altarelli-Parisi counter-terms)]
    - ★ final state [cancelled by loop IR contr.]
- Virtual (loop) contribution
  - Ultraviolet divergences: [removed by renormalisation]
  - Infrared divergences: [cancelled by real Infrared contribution]

[The quark and antiquark attached to the blob are taken as on-shell and their relative velocity v is set to zero.]

Part I

Photoproduction at mid and high P_T at HERA

Different contributions in the CSM up to NLO

NLO*: **C.Flore, J.-P. Lansberg, H.S. Shao, Y. Yedelkina, PLB 811 (2020) 135926**

Different contributions in the CSM up to NLO

NLO*: **C.Flore, J.-P. Lansberg, H.S. Shao, Y. Yedelkina, PLB 811 (2020) 135926**

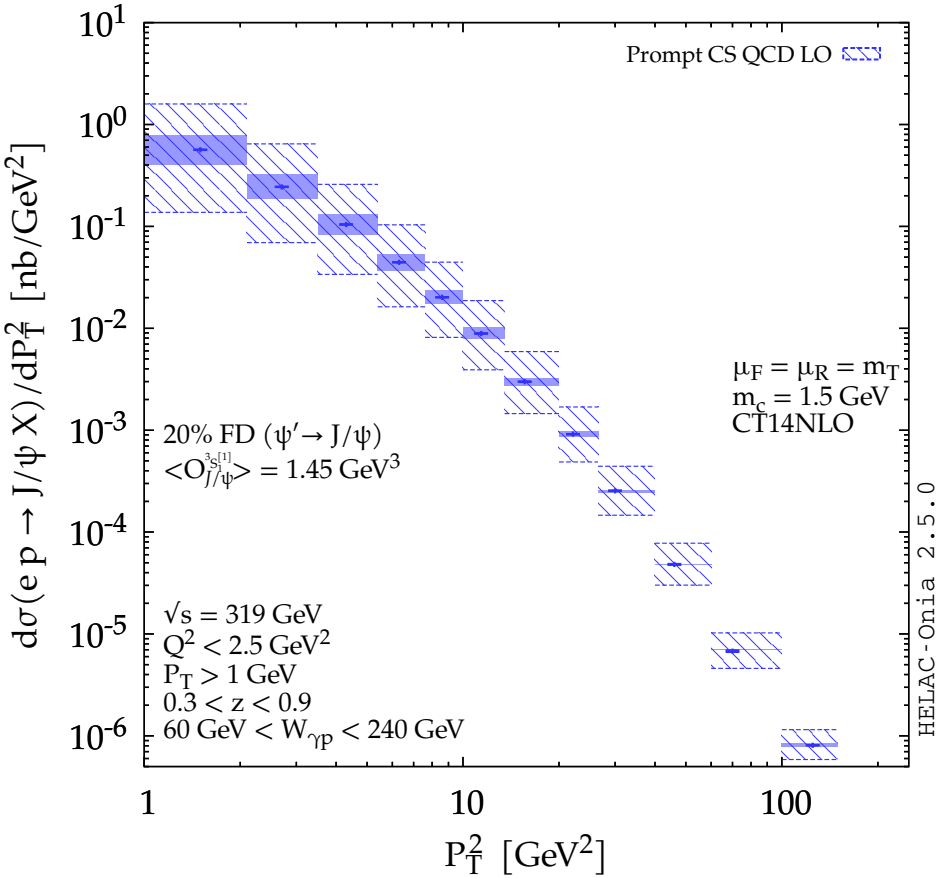

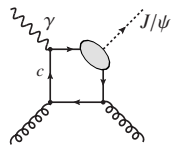

$\gamma + g \to \psi + g \; @ \; \alpha\alpha_s^2$

Notes:
The computations were done with HELAC-ONIA and FDC. The scale and mass uncertainties are shown by the hatched and solid bands. HELAC-Onia: **H.S. Shao, CPC198 (2016) 238; FDC: J.-X. Wang Nucl.Instrum.Meth. A534(2004)241-245**; See also `https://nloaccess.in2p3.fr`

Different contributions in the CSM up to NLO

NLO*: **C.Flore, J.-P. Lansberg, H.S. Shao, Y. Yedelkina, PLB 811 (2020) 135926**

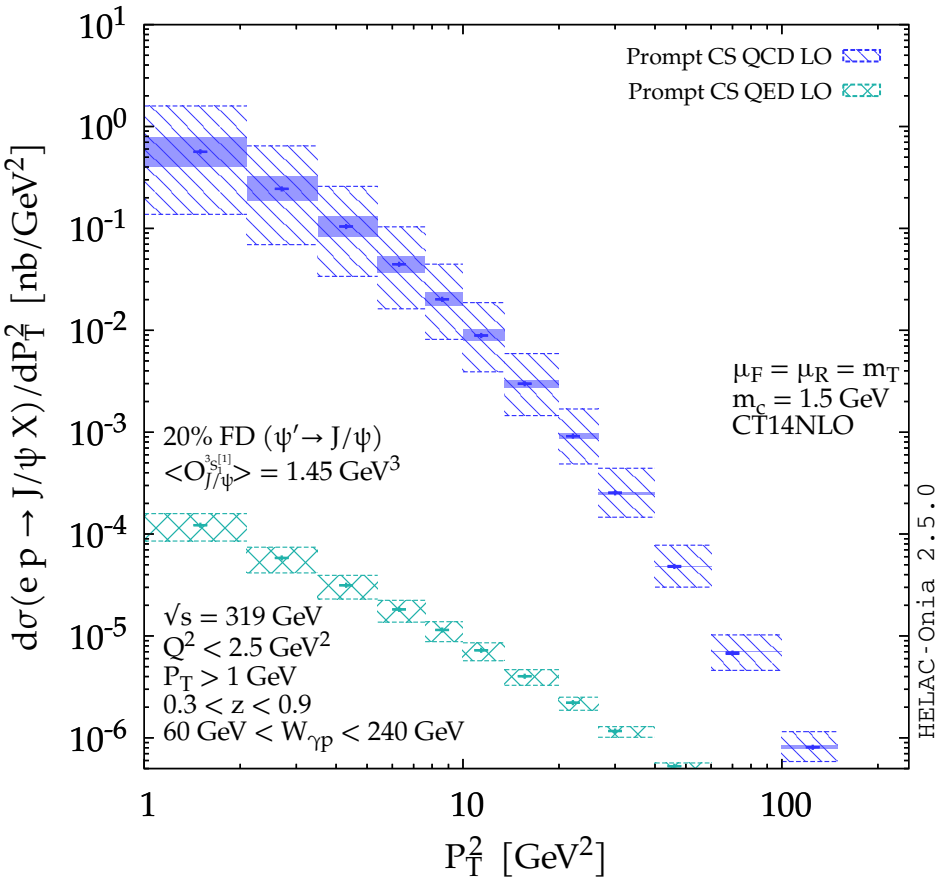

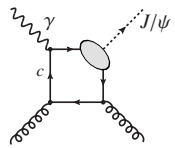

$\gamma + g \to \psi + g \; @ \; \alpha\alpha_s^2$

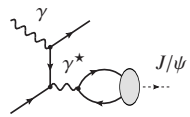

$\gamma + q \to \psi + q \; @ \; \alpha^3$ [NEW !]

Notes:
The computations were done with HELAC-ONIA and FDC. The scale and mass uncertainties are shown by the hatched and solid bands. HELAC-Onia: **H.S. Shao, CPC198 (2016) 238; FDC: J.-X. Wang Nucl.Instrum.Meth. A534(2004)241-245**; See also `https://nloaccess.in2p3.fr`

Different contributions in the CSM up to NLO

NLO*: **C.Flore, J.-P. Lansberg, H.S. Shao, Y. Yedelkina, PLB 811 (2020) 135926**

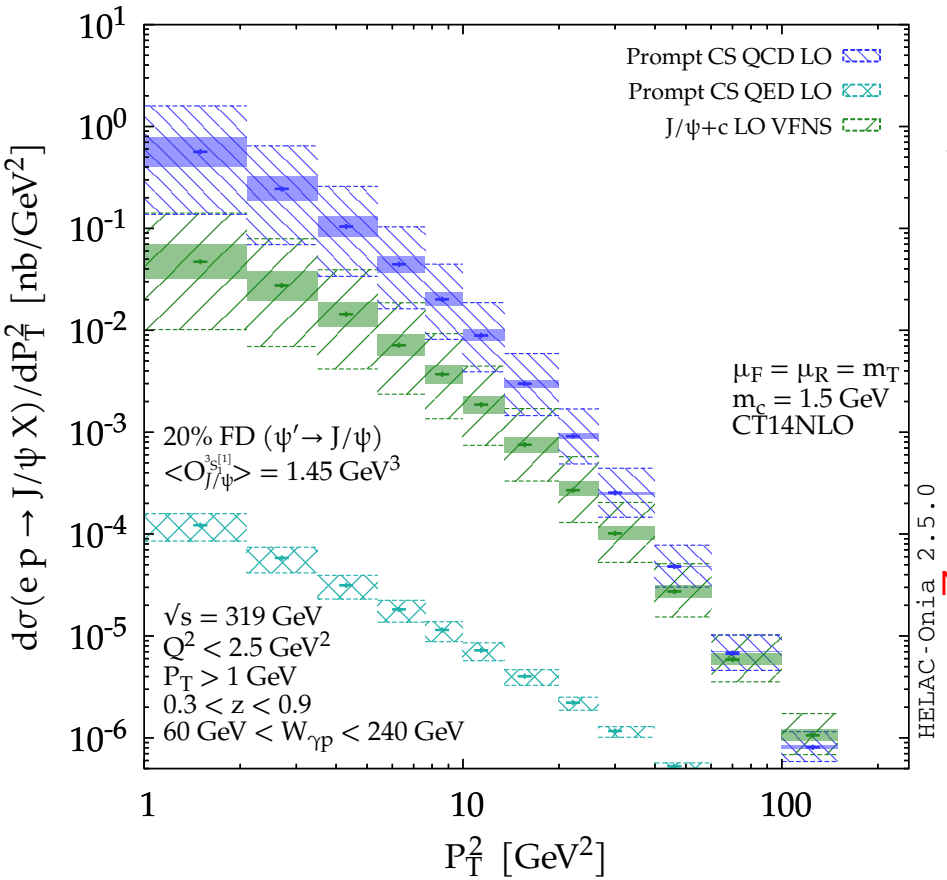

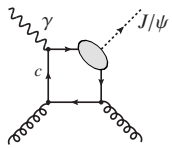

$\gamma + g \to \psi + g \,@\, \alpha\alpha_s^2$

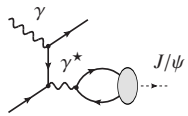

$\gamma + q \to \psi + q \,@\, \alpha^3$ [NEW !]

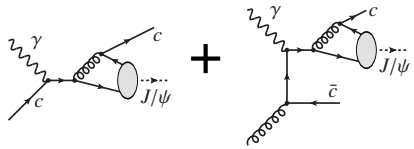

$\begin{cases} \gamma + c \to \psi + c \,@\, \alpha\alpha_s^2 \text{w. 4 Flavour Scheme} \\ \gamma + g \to \psi + c + \bar{c} \,@\, \alpha\alpha_s^3 \text{w. 3 Flavour Scheme} \end{cases}$

NLO with $K \approx 1.6$: Qi-M. Feng, C.-F. Qiao, 2405.05683 [hep-ph]

VFNS [also NEW !]

Notes:
The computations were done with HELAC-ONIA and FDC. The scale and mass uncertainties are shown by the hatched and solid bands. HELAC-Onia: **H.S. Shao, CPC198 (2016) 238; FDC: J.-X. Wang Nucl.Instrum.Meth. A534(2004)241-245**; See also `https://nloaccess.in2p3.fr`

Different contributions in the CSM up to NLO

NLO*: **C.Flore, J.-P. Lansberg, H.S. Shao, Y. Yedelkina, PLB 811 (2020) 135926**

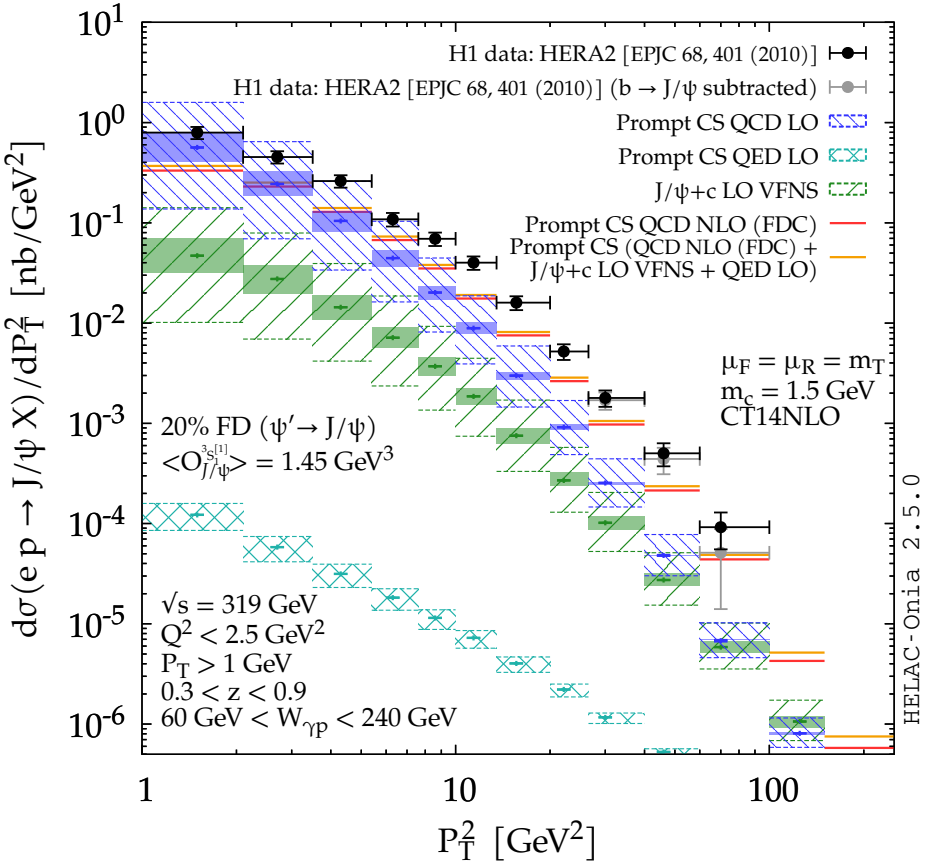

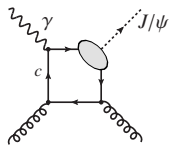

$\gamma + g \to \psi + g \,@\, \alpha\alpha_s^2$

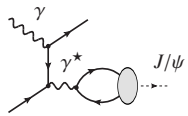

$\gamma + q \to \psi + q \,@\, \alpha^3$ [NEW !]

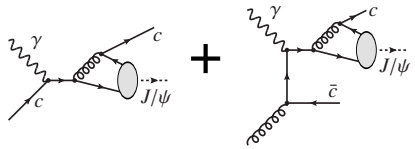

$\begin{cases} \gamma + c \to \psi + c \,@\, \alpha\alpha_s^2 \text{w. 4 Flavour Scheme} \\ \gamma + g \to \psi + c + \bar{c} \,@\, \alpha\alpha_s^3 \text{w. 3 Flavour Scheme} \end{cases}$

NLO with $K \approx 1.6$: Qi-M. Feng, C.-F. Qiao, 2405.05683 [hep-ph]

VFNS [also NEW !]

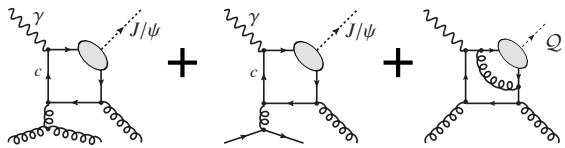

$\begin{cases} \gamma + g \to \psi + g + g \,@\, \alpha\alpha_s^3 \\ \gamma + q \to \psi + g + q \,@\, \alpha\alpha_s^3 \end{cases}$ [+ $\gamma g \to \psi g$ @ 1L]

Notes:
The computations were done with HELAC-ONIA and FDC. The scale and mass uncertainties are shown by the hatched and solid bands. HELAC-Onia: **H.S. Shao, CPC198 (2016) 238; FDC: J.-X. Wang Nucl.Instrum.Meth. A534(2004)241-245**; See also `https://nloaccess.in2p3.fr`

Different contributions in the CSM up to NLO

NLO*: **C.Flore, J.-P. Lansberg, H.S. Shao, Y. Yedelkina, PLB 811 (2020) 135926**

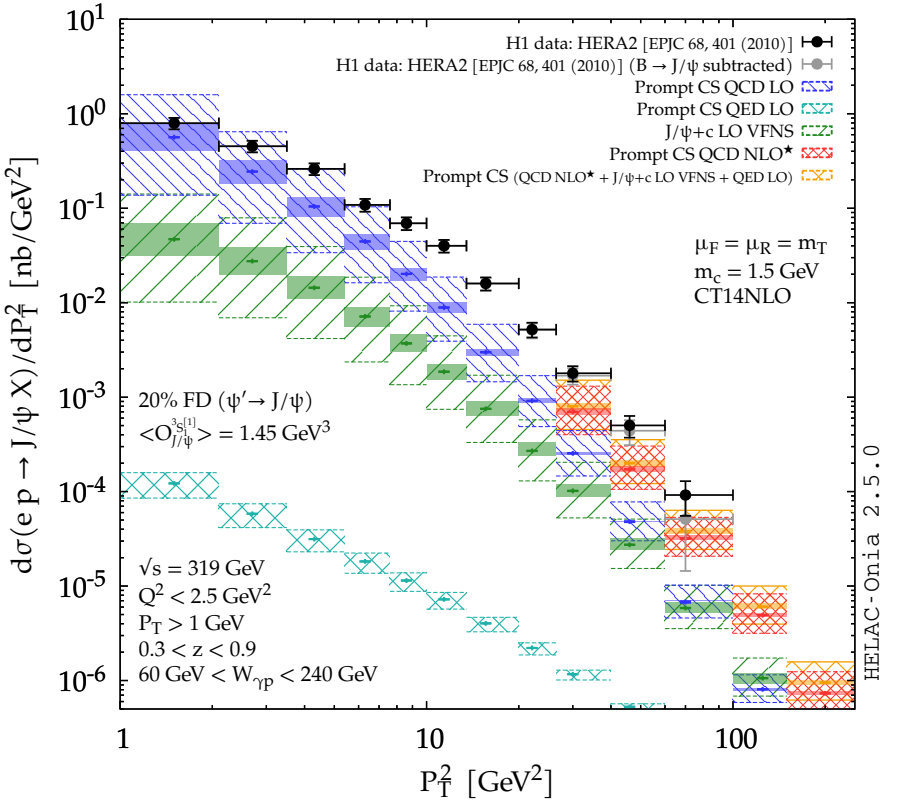

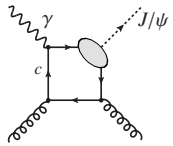

$\gamma + g \to \psi + g \,@\, \alpha\alpha_s^2$

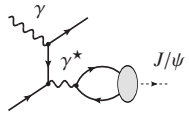

$\gamma + q \to \psi + q \,@\, \alpha^3$ [NEW !]

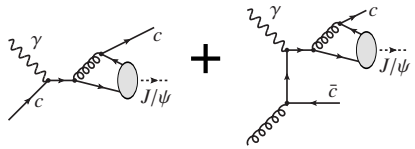

$$\begin{cases} \gamma+c\to\psi+c \,@\, \alpha\alpha_s^2 \text{w. 4 Flavour Scheme} \\ \gamma+g\to\psi+c+\bar{c} \,@\, \alpha\alpha_s^3 \text{w. 3 Flavour Scheme} \end{cases}$$

NLO with $K \approx 1.6$: Qi-M. Feng, C.-F. Qiao, 2405.05683 [hep-ph]

VFNS [also NEW !]

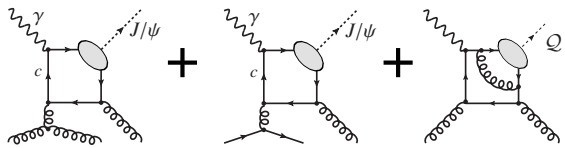

$$\begin{cases} \gamma+g\to\psi+g+g \,@\, \alpha\alpha_s^3 \\ \gamma+q\to\psi+g+q \,@\, \alpha\alpha_s^3 \end{cases} [+ \gamma g \to \psi g \text{ @ 1L}]$$

Notes:
The computations were done with HELAC-ONIA and FDC. The scale and mass uncertainties are shown by the hatched and solid bands. HELAC-Onia: **H.S. Shao, CPC198 (2016) 238; FDC: J.-X. Wang Nucl.Instrum.Meth. A534(2004)241-245**; See also `https://nloaccess.in2p3.fr`

Part II

Photoproduction at mid and high P_T at the Electron-Ion Collider

Predictions for the EIC : $J/\psi + X$ ($\sqrt{s_{ep}} = 45$ GeV)

C.Flore, J.-P. Lansberg, H.S. Shao, Y. Yedelkina, PLB 811 (2020) 135926

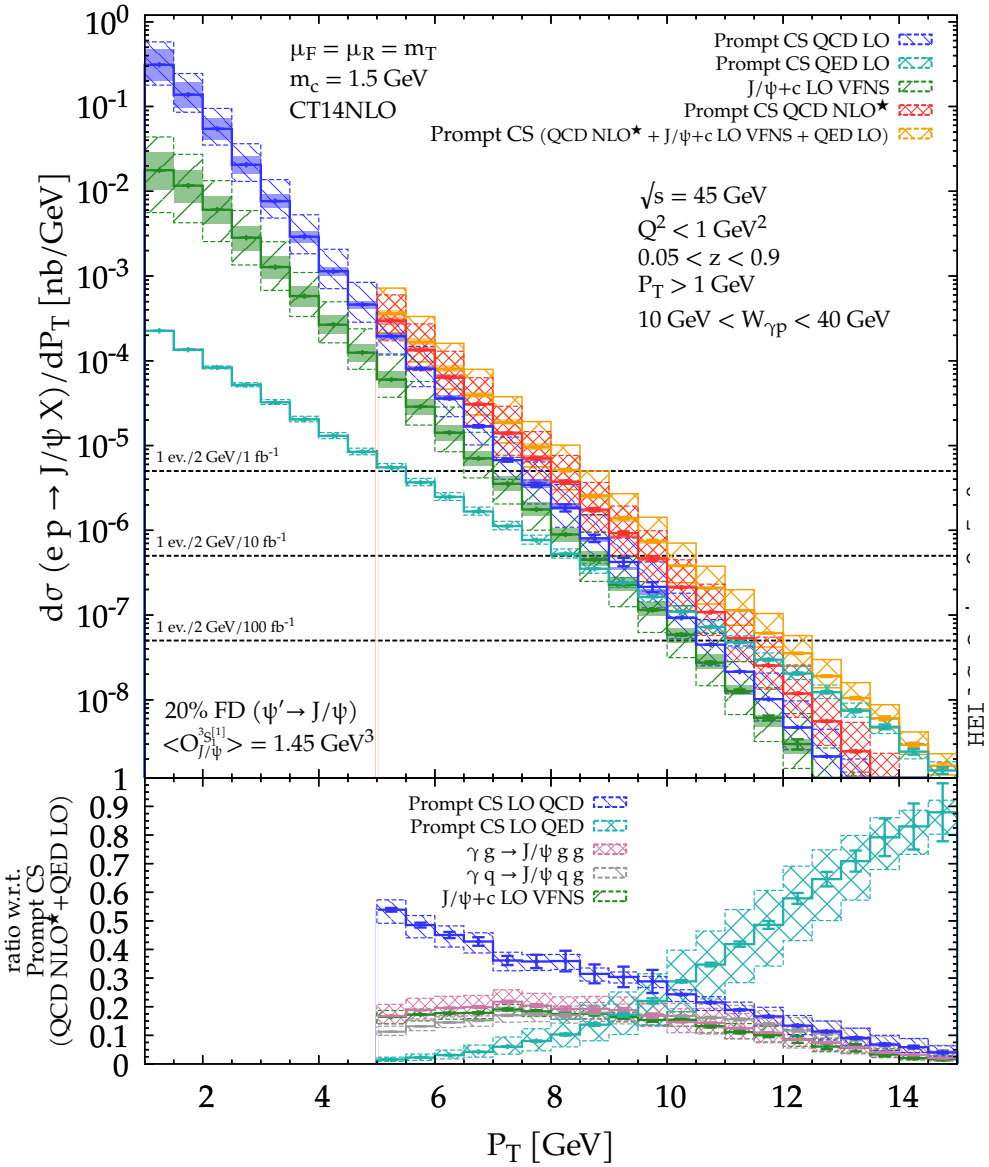

- At $\sqrt{s_{ep}} = 45$ GeV, one gets into valence region
- Yield steeply falling with P_T
- Yield can be measured up to $P_T \sim 11$ GeV with $\mathcal{L} = 100$ fb^{-1}

  [using both *ee* and $\mu\mu$ decay channels and $\varepsilon_{J/\psi} \simeq 80\%$]
- QED contribution leading at the largest reachable P_T
- photon-quark fusion contributes more than 30 % for $P_T > 8$ GeV

Predictions for the EIC : $J/\psi + X$ ($\sqrt{s_{ep}} = 140$ GeV)

C.Flore, J.-P. Lansberg, H.S. Shao, Y. Yedelkina, PLB 811 (2020) 135926

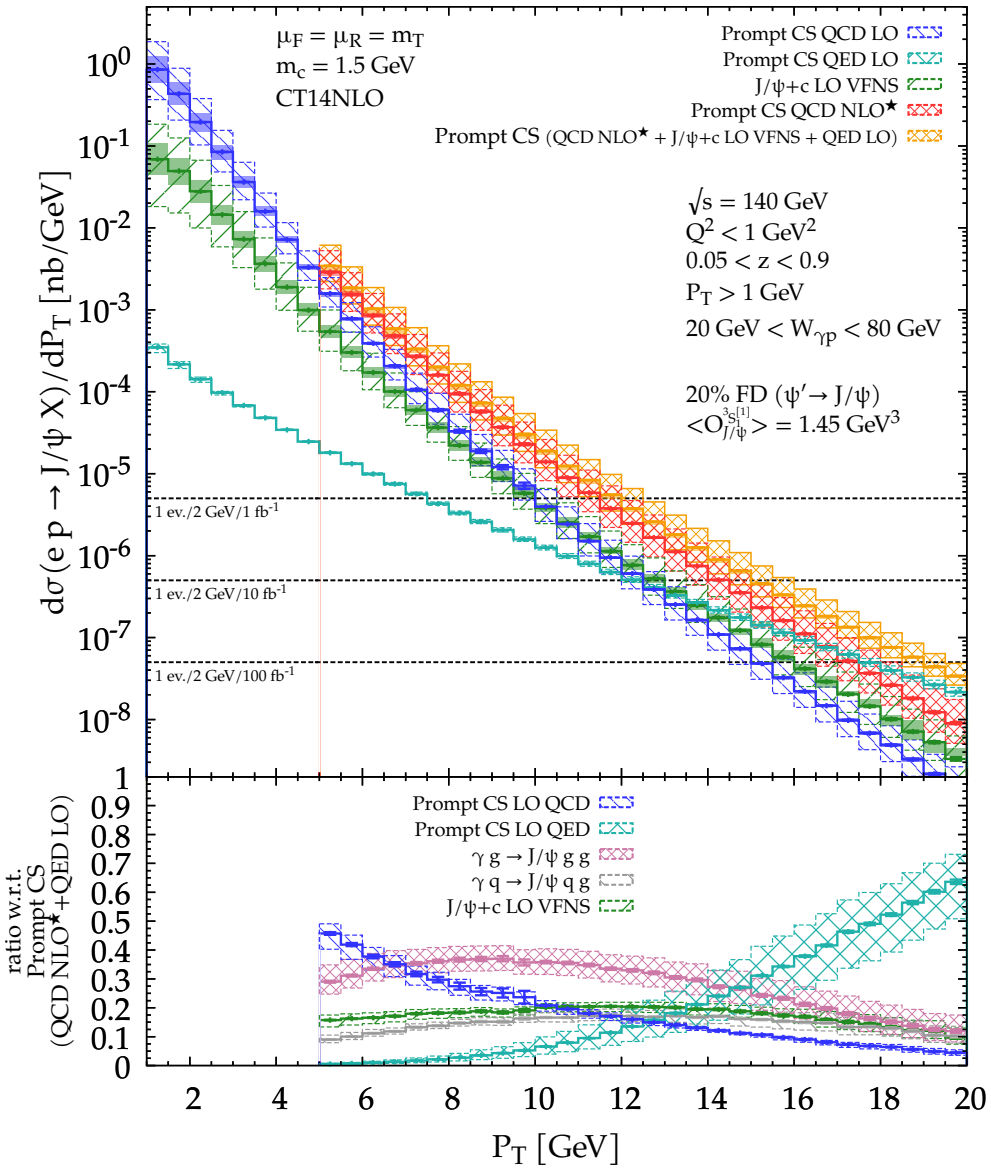

- At $\sqrt{s_{ep}} = 140$ GeV, larger P_T range up to approx. 18 GeV
- QED contribution also leading at the largest reachable P_T
- photon-gluon fusion contributions dominant up to approx. 15 GeV
- $J/\psi + 2$ hard partons [*i.e.* $J/\psi + \{gg, qg, c\bar{c}\}$] dominant for $P_T \sim 8 - 15$ GeV
- It could lead to the observation of $J/\psi + 2$ jets with moderate P_T^{jet}
- with a specific topology where the leading jet_1 recoils on the $J/\psi + \text{jet}_2$ pair

Part III

J/ψ+charm associated production at the EIC

J/ψ+charm associated production at the EIC

C.Flore, J.-P. Lansberg, H.S. Shao, Y. Yedelkina, PLB 811 (2020) 135926

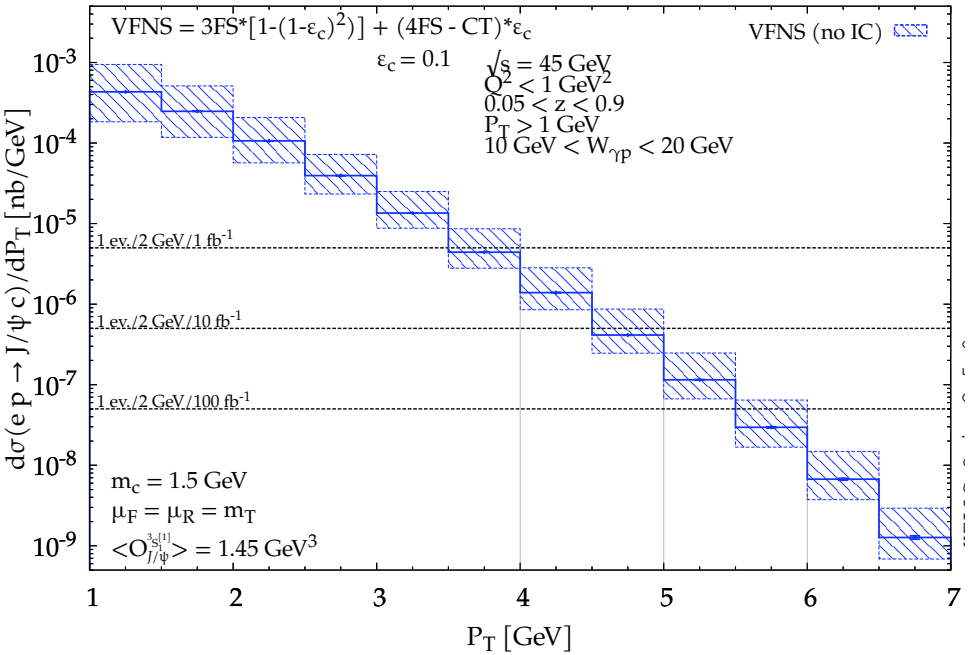

- Same LO VFNS computation previously shown in green except for the charm-detection efficiency ϵ_c: $\sigma^{VFNS} = \sigma^{3FS} \times (1-(1-\epsilon)^2) + (\sigma^{4FS} - \sigma^{CT}) \times \epsilon$
- At $\sqrt{s_{ep}} = 45$ GeV, yield limited to low P_T even with $\mathcal{L} = 100$ fb^{-1}
- But it is clearly observable if $\epsilon_c = 0.1$ with $\mathcal{O}(5000, 500, 50)$ events for $\mathcal{L} = (100, 10, 1)$ fb^{-1}

J/ψ+charm associated production at the EIC

C.Flore, J.-P. Lansberg, H.S. Shao, Y. Yedelkina, PLB 811 (2020) 135926

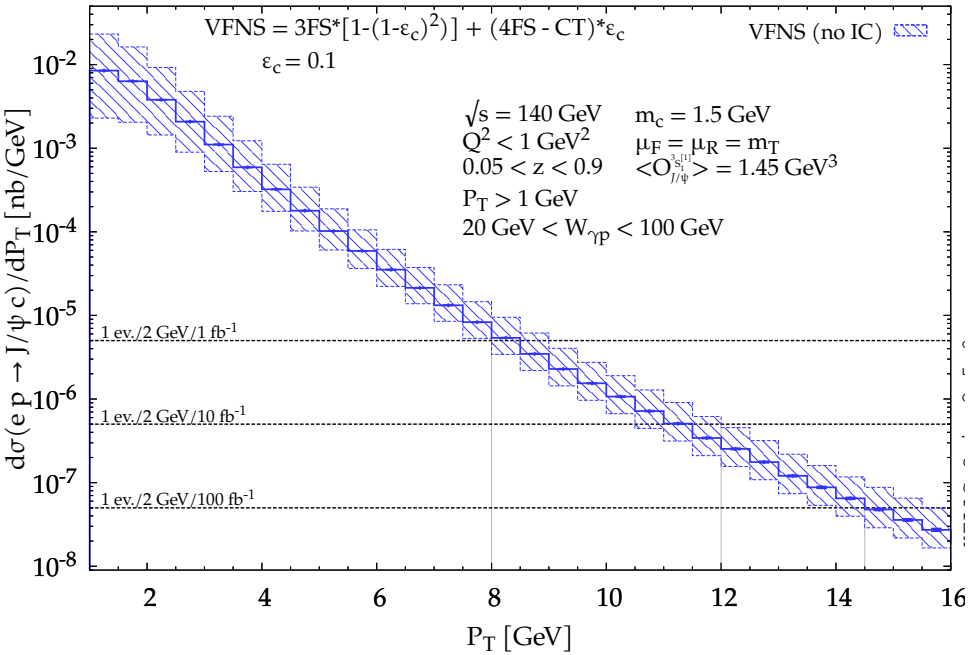

- Same LO VFNS computation previously shown in green except for the charm-detection efficiency ϵ_c: $\sigma^{VFNS} = \sigma^{3FS} \times (1-(1-\epsilon)^2) + (\sigma^{4FS} - \sigma^{CT}) \times \epsilon$
- At $\sqrt{s_{ep}} = 45$ GeV, yield limited to low P_T even with $\mathcal{L} = 100$ fb^{-1}
- But it is clearly observable if $\epsilon_c = 0.1$ with $\mathcal{O}(5000, 500, 50)$ events for $\mathcal{L} = (100, 10, 1)$ fb^{-1}
- At $\sqrt{s_{ep}} = 140$ GeV, P_T range up to 13-14 GeV with up to order 10^4 of events with $\mathcal{L} = 100$ fb^{-1}
- Could be observed via charm jet

J/ψ+charm associated production at the EIC

C.Flore, J.-P. Lansberg, H.S. Shao, Y. Yedelkina, PLB 811 (2020) 135926

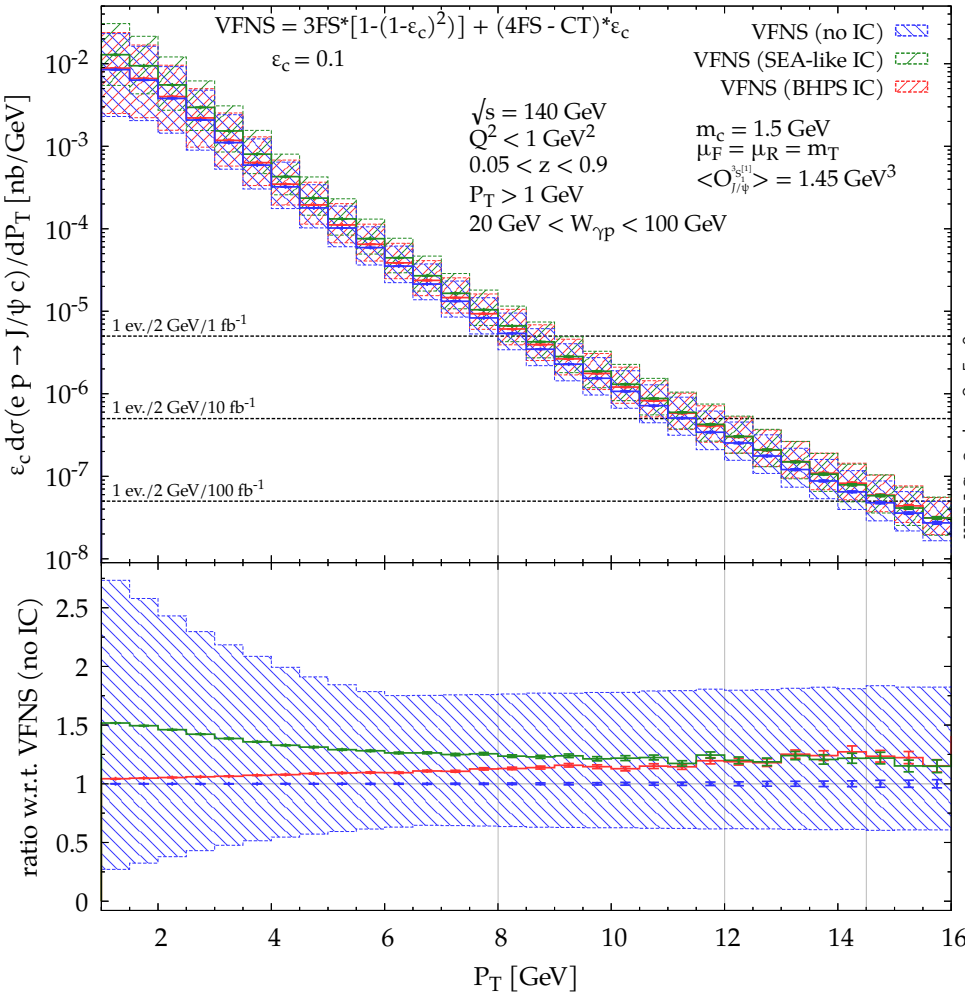

- Same LO VFNS computation previously shown in green except for the charm-detection efficiency ϵ_c: $\sigma^{VFNS} = \sigma^{3FS} \times (1-(1-\epsilon)^2) + (\sigma^{4FS} - \sigma^{CT}) \times \epsilon$
- At $\sqrt{s_{ep}} = 45$ GeV, yield limited to low P_T even with $\mathcal{L} = 100$ fb^{-1}
- But it is clearly observable if $\epsilon_c = 0.1$ with $\mathcal{O}(5000, 500, 50)$ events for $\mathcal{L} = (100, 10, 1)$ fb^{-1}
- At $\sqrt{s_{ep}} = 140$ GeV, P_T range up to 13-14 GeV with up to order 10^4 of events with $\mathcal{L} = 100$ fb^{-1}
- Could be observed via charm jet

- 4FS $\gamma c \to J/\psi c$ depend on $c(x)$ and could be enhanced by intrinsic charm
- Small effect at $\sqrt{s_{ep}} = 140$ GeV

[We used IC $c(x)$ encoded in CT14NNLO]

J/ψ+charm associated production at the EIC

C.Flore, J.-P. Lansberg, H.S. Shao, Y. Yedelkina, PLB 811 (2020) 135926

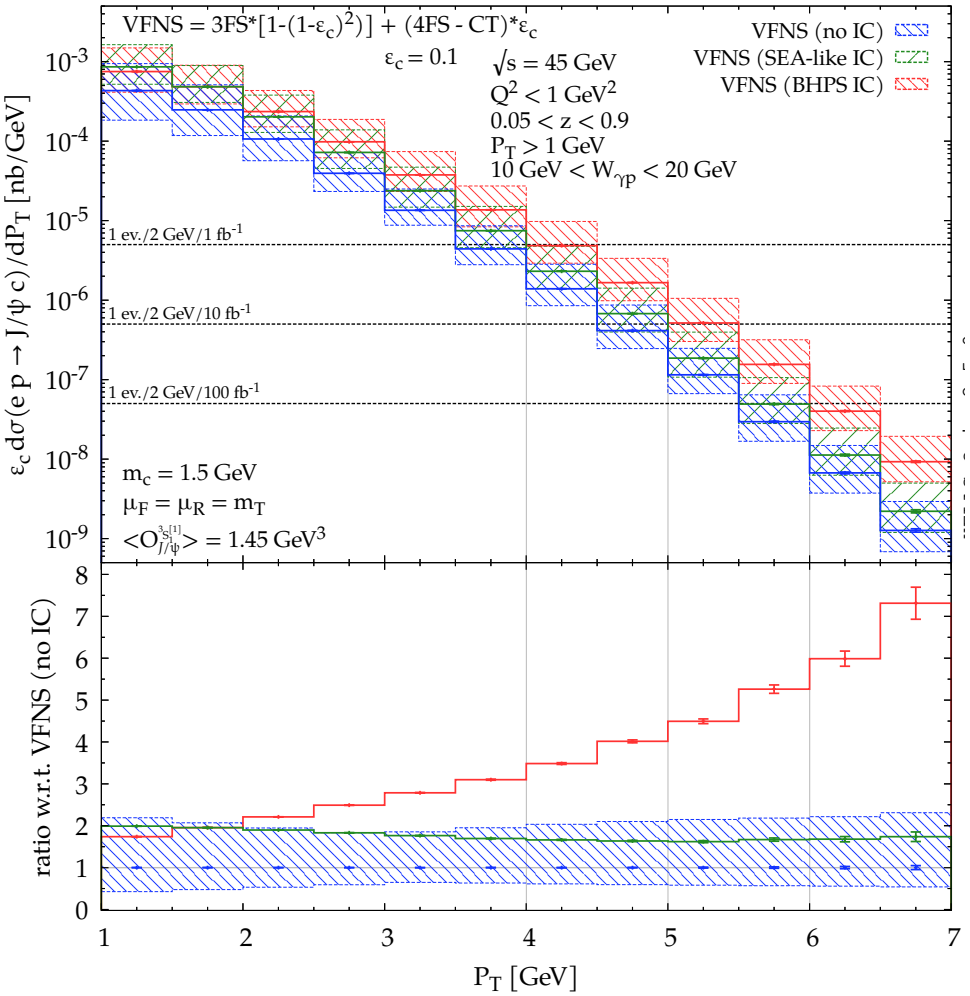

- Same LO VFNS computation previously shown in green except for the charm-detection efficiency ϵ_c: $\sigma^{VFNS} = \sigma^{3FS} \times (1-(1-\epsilon)^2) + (\sigma^{4FS} - \sigma^{CT}) \times \epsilon$
- At $\sqrt{s_{ep}} = 45$ GeV, yield limited to low P_T even with $\mathcal{L} = 100$ fb^{-1}
- But it is clearly observable if $\epsilon_c = 0.1$ with $\mathcal{O}(5000, 500, 50)$ events for $\mathcal{L} = (100, 10, 1)$ fb^{-1}
- At $\sqrt{s_{ep}} = 140$ GeV, P_T range up to 13-14 GeV with up to order 10^4 of events with $\mathcal{L} = 100$ fb^{-1}
- Could be observed via charm jet

- 4FS $\gamma c \to J/\psi c$ depend on $c(x)$ and could be enhanced by intrinsic charm
- Small effect at $\sqrt{s_{ep}} = 140$ GeV [We used IC $c(x)$ encoded in CT14NNLO]
- Measurable effect at $\sqrt{s_{ep}} = 45$ GeV: BHPS valence-like peak visible !

Part IV

Study of the impact of the NLO corrections to P_T-integrated photoproduction cross section

Squared amplitude

expected soon on NLOAccess !

- FeynArts: to generate expressions for Feynman diagrams with Colour Singlet spin projector:

$$c(p_1) + \bar{c}(p_2) \to c\bar{c}\left[{}^3S_1^{(1)}\right](k_3)$$

- Virtual: FeynCalc: tensor reduction & find master topologies
- Solve linear dependence in propagators introduced with NRQCD limit → partial-fractioning
- IBP reduction of Feynman integrals to master integrals: KIRA, FIRE
- LoopTools+HypExp library: Feynman integrals are evaluated in an efficient and numerically-stable way
- UV renormalisation
- Real: $2 \to 3$ amplitudes with FormCalc
- The Catani-Seymour Dipole subtraction terms:
  1. $2 \to 3$ dipole term to subtract from the real contribution → finite + numerical ph-sp integration
  2. add $2 \to 2$ integrated-dipole term to the virtual contribution
- Altarelli-Parisi counter-term (absorbs initial-emission collinear singularities into factorised PDFs of photon)
- Fortran (CUBA): phase-space (MC) integration
- Cross checks against other existing implementations (thanks to **M. Butenschoen, Yu Feng, C. Flore**)

The scaling functions

J.P. Lansberg, M.Nefedov, Y. Yedelkina: PoS EPS-HEP2023 (2024) 271

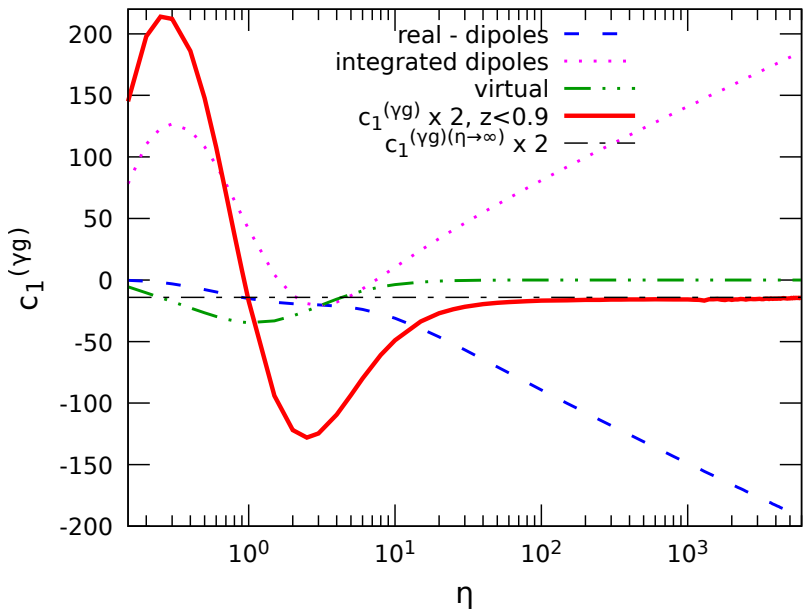

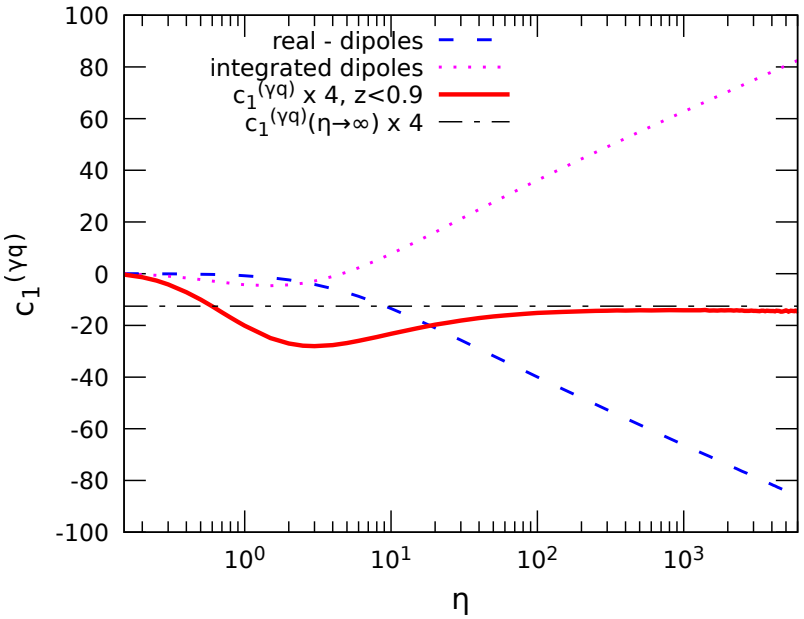

$$\eta = \frac{\hat{s} - M^2}{M^2};\ z = \frac{k_3 k_2}{k_1 k_2};\ \rho = \frac{|\mathbf{k}_{T3}|^2}{M^2};\ F_{LO} = \frac{16\alpha\alpha_s^2 e_Q^2}{9M^2} \frac{\langle \mathcal{O}\left[{}^3S_1^{(1)}\right]\rangle}{M^3} \tag{1}$$

$$\frac{d\hat{\sigma}^{\rm CSM}_{\gamma i}}{dz d\rho} = F_{LO}\left\{ \frac{dc_0}{dz d\rho}\delta_{gi} + \frac{\alpha_s}{2\pi}\left[\beta_0(n_{1f})\frac{dc_0}{dz d\rho}\ln\frac{\mu_R^2}{\mu_F^2}\delta_{gi}\right.\right. \tag{2}$$

$$\left.\left. + \frac{dc_1^{(\gamma i)}(\eta,\rho,z)}{dz d\rho} + \frac{d\bar{c}_1^{(\gamma i)}(\eta,\rho,z)}{dz d\rho}\ln\frac{M^2}{\mu_F^2}\right]\right\}_{i=g,q} \tag{3}$$

The negative cross-sections issue at high energies

A. Colpani Serri, Y. Feng, C. Flore, J.P. Lansberg, M.A. Ozcelik, H.S. Shao, Y. Yedelkina: arXiv:2112.05060 [hep-ph]

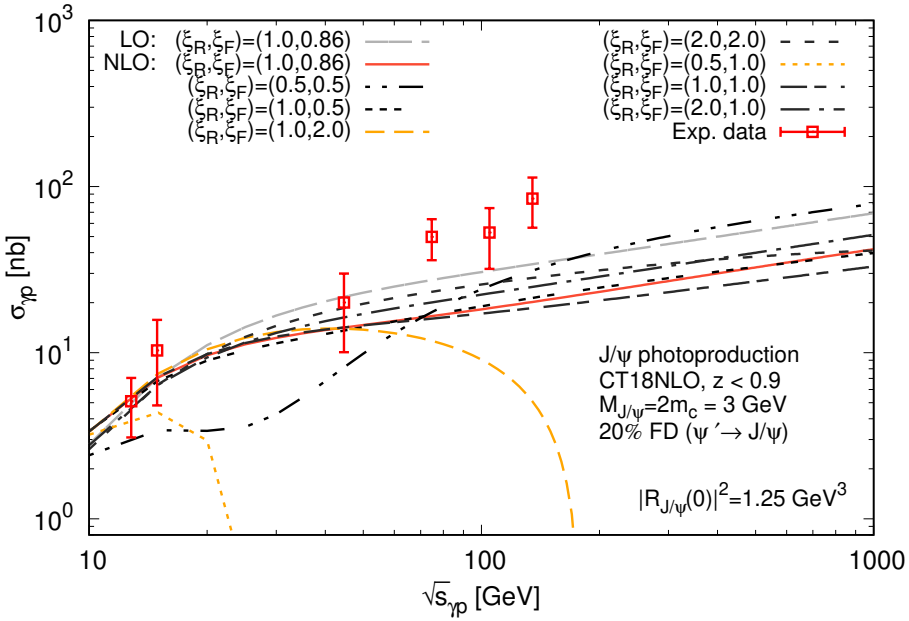

- NLO cross section for J/ψ photoproduction becomes negative for large μ_F when $\sqrt{s_{\gamma p}}$ increases
- For $\mu_F = 2M$, $\sigma < 0$ as in case of η_c hadroproduction

J.P. Lansberg, M.A. Ozcelik: Eur.Phys.J.C 81 (2021) 6, 497

- 2 possible sources of negative partonic cross sections: loop corrections (interference) and from real emission (subtraction of IR poles)

Exp. data: H1 - M.Kraemer: NPB 459(1996)3-50, FTPS - B.H.Denby et al.: PRL 52(1984)795-798, NAI - NA14Collaboration, R.Barate et al.:Z.Phys.C 33(1987)505

Negative cross-section values

A. Colpani Serri, Y. Feng, C. Flore, J.P. Lansberg, M.A. Ozcelik, H.S. Shao, Y. Yedelkina: arXiv:2112.05060 [hep-ph]

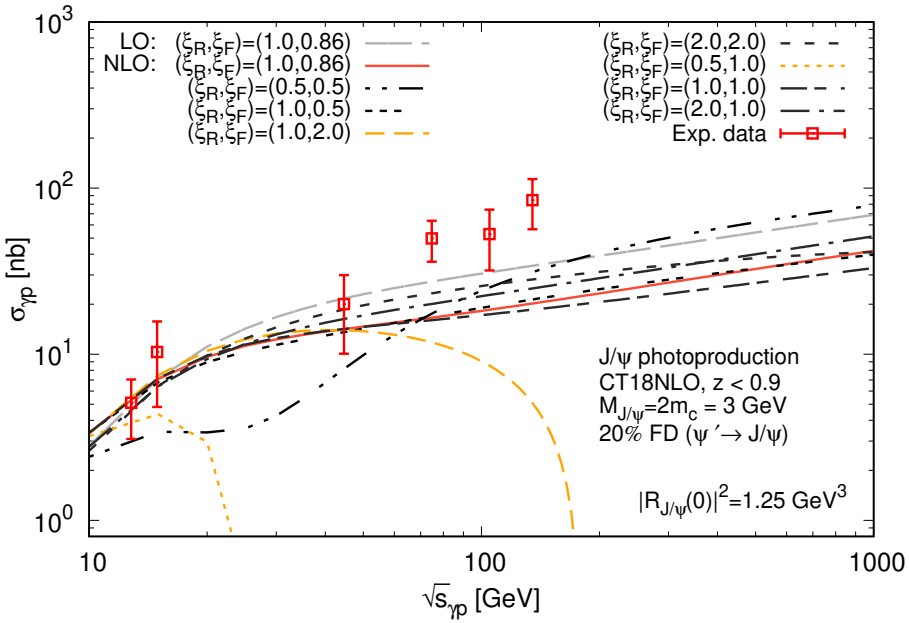

- Initial state collinear divergences are removed via the subtraction into the PDFs via AP-CT
- $\hat{s} \to \infty : \ \hat{\sigma}_{\gamma i}^{NLO} \propto \alpha_s(\mu_R) \left(\bar{c}_1^{(\gamma i)} \log \frac{M_Q^2}{\mu_F^2} + c_1^{(\gamma i)} \right), A_{\gamma i} = \frac{c_1^{(\gamma i)}}{\bar{c}_1^{(\gamma i)}},$

$$\boxed{A_{\gamma g} = A_{\gamma q}}$$

A scale prescription for μ_F

J.P. Lansberg, M.A. Ozcelik: Eur.Phys.J.C 81 (2021) 6, 497

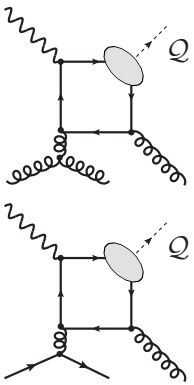

- In principle, such negative terms should be compensated by the evolution of the PDFs governed by the DGLAP equations;
- $A_{\gamma g}, A_{\gamma q}$ are process-dependent, while the DGLAP equations are process-independent, which makes the compensation imperfect;
- But as $A_{\gamma g} = A_{\gamma q}$, we can choose μ_F such that $lim_{\hat{s}\to\infty}\hat{\sigma}^{NLO}_{\gamma i} = 0$
- This amounts to consider that all the QCD corrections are in the PDFs
- The choice of factorisation scale to avoid possible negative hadronic cross-section: (for η_Q : $A_{gi} = -1$) $\mu_F = \hat{\mu}_F = Me^{A_{\gamma i}/2}$;
- For J/ψ (Υ) photoproduction: $\hat{\mu}_F \approx 0.86M$ ($P_T \in [0, \infty]$, $z < 0.9$)

Results with $\hat{\mu}_F = 0.85M$

A. Colpani Serri, Y. Feng, C. Flore, J.P. Lansberg, M.A. Ozcelik, H.S. Shao, Y. Yedelkina: arXiv:2112.05060 [hep-ph]

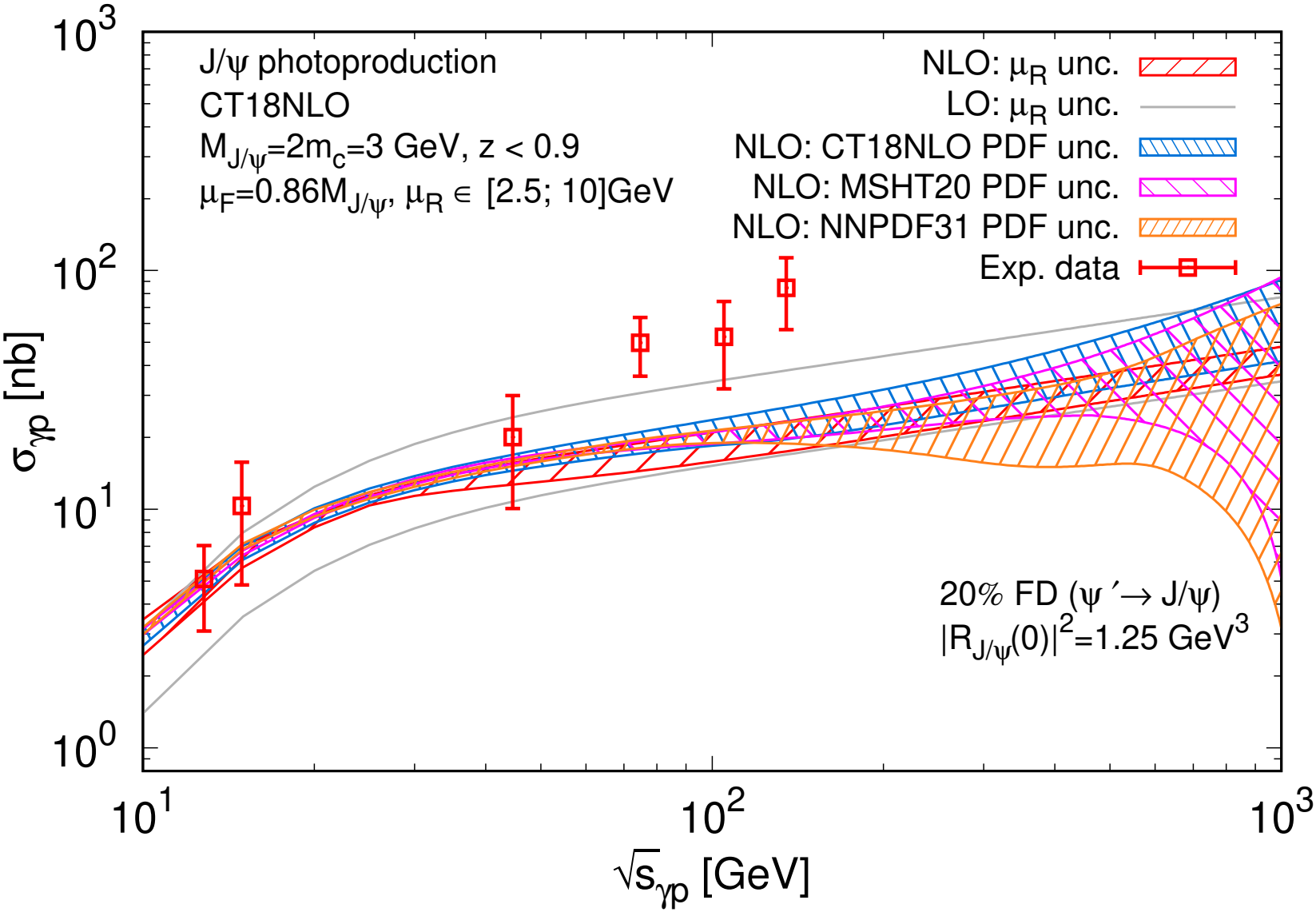

Exp. data: H1 - M.Kraemer: Nucl.Phys.B 459(1996)3-50, FTPS - B.H.Denbyet al.: Phys.Rev.Lett. 52(1984)795-798, NAI - NA14Collaboration, R.Barateet al.:Z.Phys.C 33(1987)505

P_T-differential cross sections

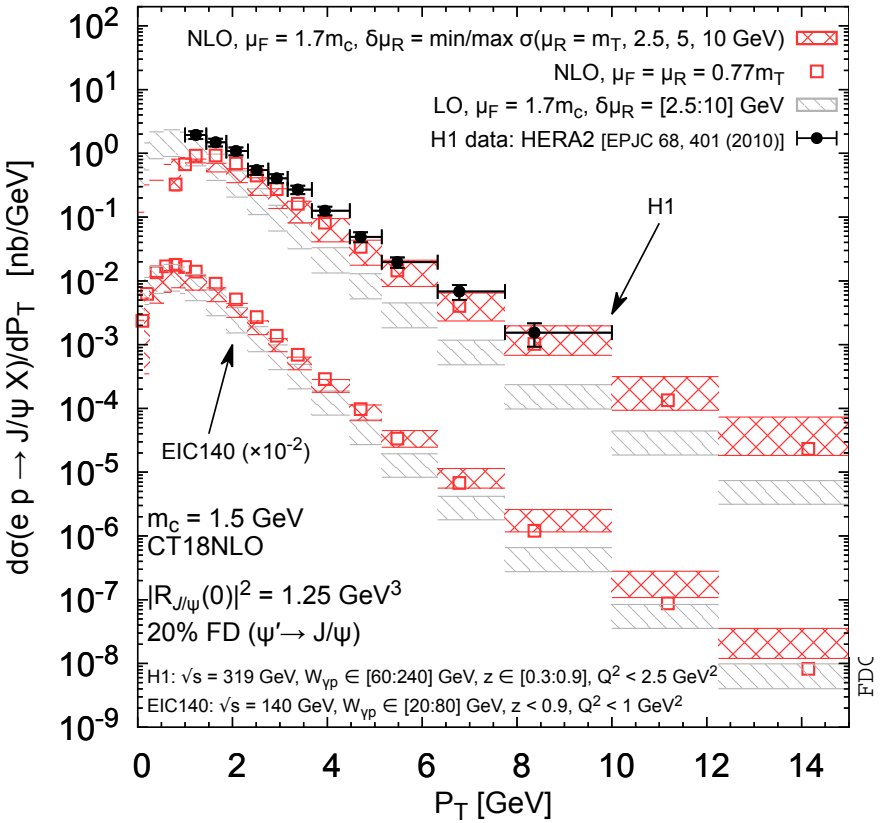

- If p_T-dependence is taken into account, for $\hat{s} \to \infty$:
  $c_1^{(\gamma i)}(p_T)/\overline{c}_1^{(\gamma i)}(p_T) \propto (P_T/M_Q)^2$
- $\Rightarrow \hat{\mu}_F = Me^{c_{\gamma i}^{(1)}/2\overline{c}_{\gamma i}^{(1)}} \propto Me^{P_T^2/M^2}$, which is weird
- Full matched calculation between NLO and $\ln \hat{s}/M^2$-resummation is needed
- Common dynamical scale choice: $\mu_F = (0.5, 1, 2)m_T$

- one can use $\mu_F = \alpha\sqrt{M^2 + P_T^2}$ or $\mu_F = \sqrt{(\beta M)^2 + P_T^2}$
- if P_T is large, then $\mu_F \propto P_T$
- For $\mu_F = \hat{\mu}_F$ with $< P_T^2 >= 2.5\text{GeV}^2$ (for J/ψ at HERA energies), we get $\alpha = 0.77$ and $\beta = 0.7$

Part V

Can J/ψ & Υ allow us to probe PDFs? : PDF vs scale uncertainties

J/ψ&Y: PDF uncertainties of $\sigma(\sqrt{s_{\gamma p}})$

A. Colpani Serri, Y. Feng, C. Flore, J.P. Lansberg, M.A. Ozcelik, H.S. Shao, Y. Yedelkina: arXiv:2112.05060 [hep-ph]

- PDF uncertainties increase at large $\sqrt{s}$ (i.e. small x)
- The μ_R unc. are reduced at NLO in comparison with LO

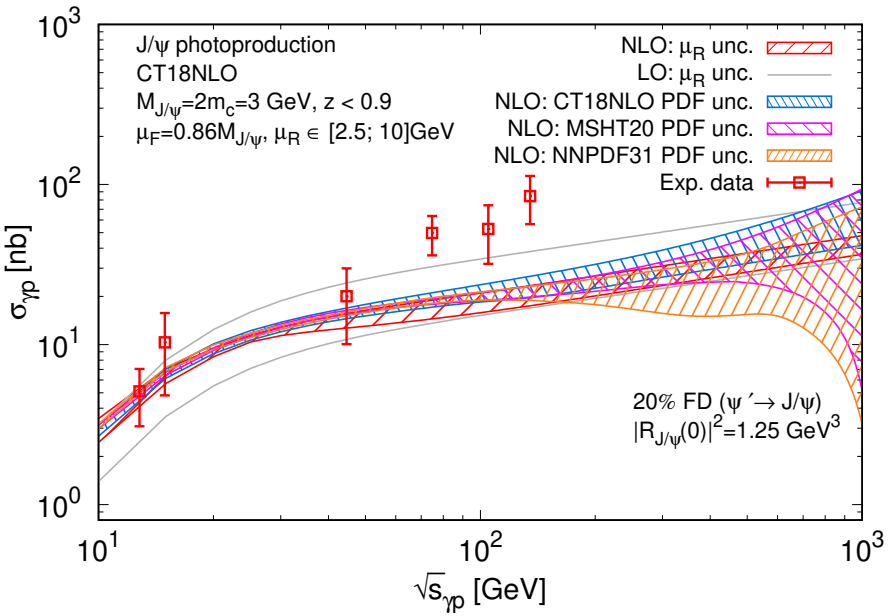

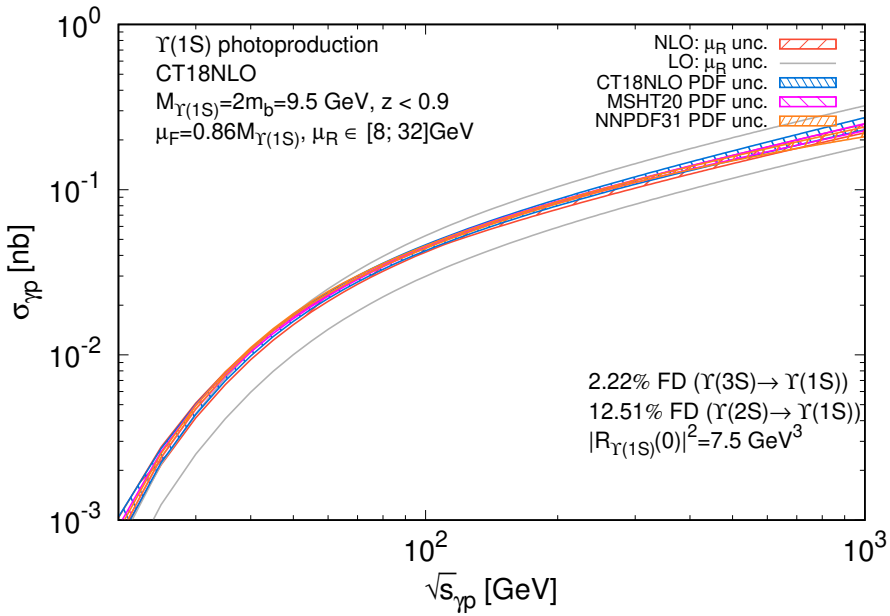

Exp. data: H1 - Nucl.Phys.B 472(1996)3-31, FTPS - B.H.Denby et al.: PRL 52(1984)795-798, NAI - NA14Collaboration, R.Barate et al.:Z.Phys.C 33(1987)505

J/ψ&Y: PDF uncertainties of $\sigma(\sqrt{s_{\gamma p}})$

A. Colpani Serri, Y. Feng, C. Flore, J.P. Lansberg, M.A. Ozcelik, H.S. Shao, Y. Yedelkina: arXiv:2112.05060 [hep-ph]

- PDF uncertainties increase at large $\sqrt{s}$ (i.e. small x)
- The μ_R unc. are reduced at NLO in comparison with LO
- Increase of μ_R unc. from $\sqrt{s_{\gamma p}} \gtrsim 50$ GeV from the loop corr.
- At NNLO we expect a further reduction of μ_R uncertainties

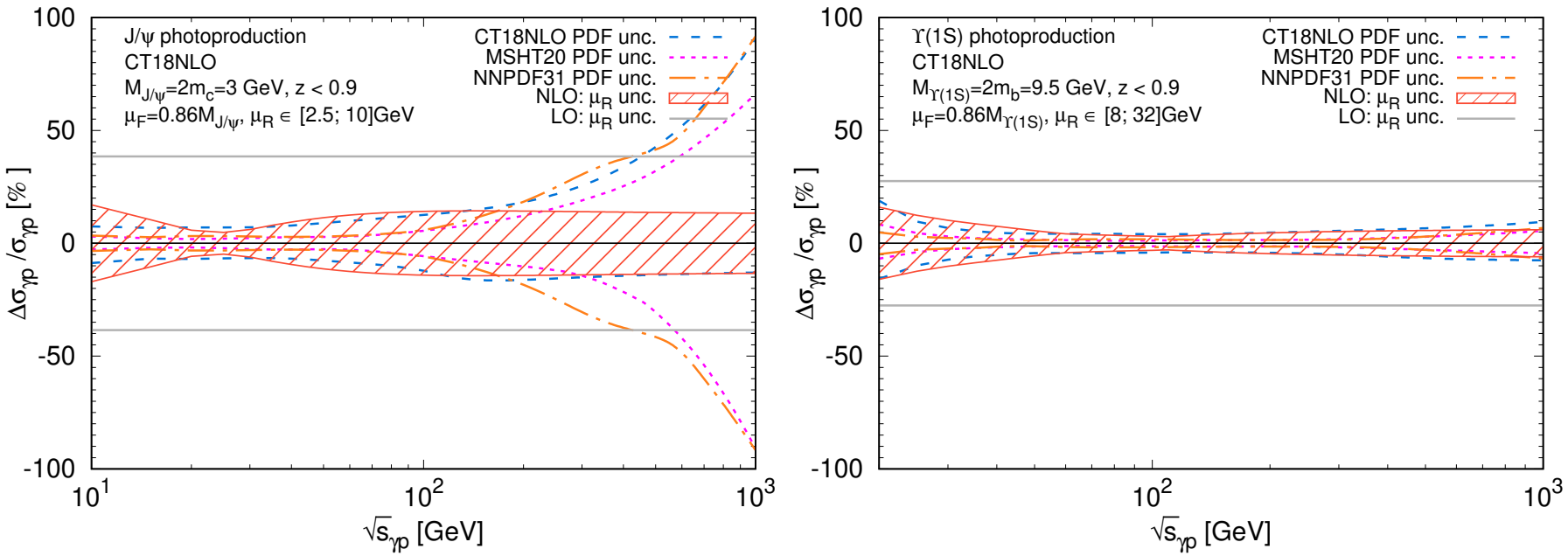

Exp. data: H1 - Nucl.Phys.B 472(1996)3-31, FTPS - B.H.Denby et al.: PRL 52(1984)795-798, NAI - NA14Collaboration, R.Barate et al.:Z.Phys.C 33(1987)505

$\sigma_{ep}(\sqrt{s})$

A. Colpani Serri, Y. Feng, C. Flore, J.P. Lansberg, M.A. Ozcelik, H.S. Shao, Y. Yedelkina: arXiv:2112.05060 [hep-ph]

Exp.	$\sqrt{s_{ep}}$	$\mathcal{L}$ (fb^{-1})	$N_{J/\psi}$	$N_{\Upsilon(1S)}$
EicC	16.7	100	$1.5^{+0.3}_{-0.2} \cdot 10^6$	$2.3^{+1.1}_{-1.4} \cdot 10^0$
AMBER	17.3	1	$1.6^{+0.3}_{-0.3} \cdot 10^4$	< 1
EIC	45	100	$8.5^{+0.5}_{-1.0} \cdot 10^6$	$6.1^{+0.7}_{-0.8} \cdot 10^2$
EIC	140	100	$2.5^{+0.1}_{-0.4} \cdot 10^7$	$7.6^{+0.3}_{-0.7} \cdot 10^3$
LheC	1183	100	$9.3^{+2.9}_{-2.9} \cdot 10^7$	$8.1^{+0.4}_{-0.7} \cdot 10^4$
FCC-eh	3464	100	$1.6^{+0.2}_{-1.0} \cdot 10^8$	$1.8^{+0.1}_{-0.2} \cdot 10^5$

We expect μ_R unc. to shrink at NNLO:
Possibility to constrain PDF with differential measurements

Rem. $N_{\psi'} \simeq 0.08 \times N_{J/\psi}$, $N_{\Upsilon(2S)} \simeq 0.4 \times N_{\Upsilon(1S)}$, $N_{\Upsilon(3S)} \simeq 0.35 \times N_{\Upsilon(1S)}$

Part VI

High-Energy factorisation and matching to NLO for inclusive quarkonium production

High-Energy Factorization

J.-Ph. Lansberg, M. Nefedov, M.A. Ozcelik, JHEP 05 (2022) 083

The **LLA** ($\sum_n \alpha_s^n \ln^{n-1}(1+\eta)$) formalism is due to [Collins, Ellis, 91'; Catani, Ciafaloni, Hautmann, 91',94'] :

$$\hat{\sigma}_{\rm HEF}(\eta) \propto \int_0^{1+\eta} \frac{dy}{y} \int_0^{\infty} d\mathbf{q}_{T1}^2 \mathcal{C}\left(\frac{y}{1+\eta}, \mathbf{q}_{T1}^2, \mu_F, \mu_R\right) \times \mathcal{H}(y, \mathbf{q}_{T1}^2) + \text{NLLA} + O(1/\eta).$$

Physical picture in the **LLA** for photoproduction:

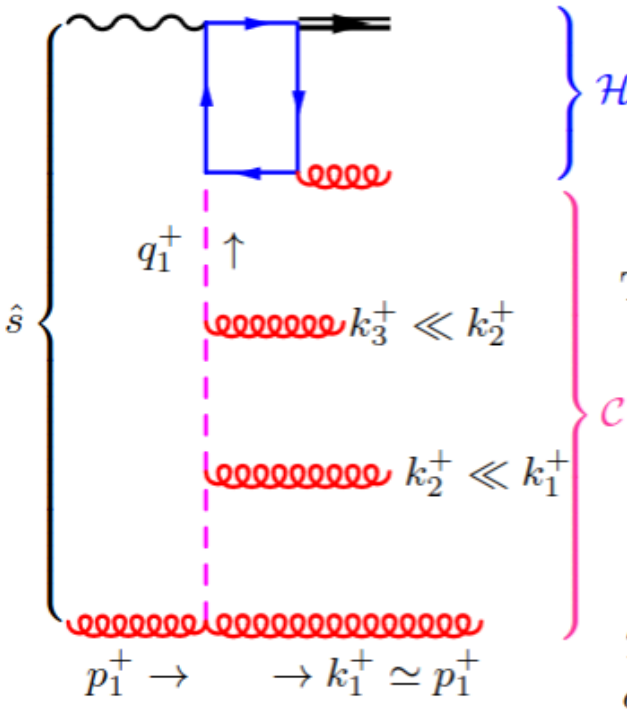

- The resummation factor $\mathcal{C}$ is the solution of the LL **BFKL** equation with collinear divergences subtracted, which resums all terms $\propto (\hat{\alpha}_s/N)^n$ (complete LLA) has the form:

$$\mathcal{C}(N, \mathbf{q}_T, \mu_F) = R(\gamma_{gg}(N, \alpha_s)) \frac{\gamma_{gg}(N,\alpha_s)}{\mathbf{q}_T^2} \left(\frac{\mathbf{q}_T^2}{\mu_F^2}\right)^{\gamma_{gg}(N,\alpha_s)},$$

- ..., where for consistency with fixed-order **DGLAP** evolution

$$\gamma_{gg}(N, \alpha_s) = \frac{\hat{\alpha}_s}{N} + 2\zeta(3)\frac{\hat{\alpha}_s^4}{N^4} + 2\zeta(5)\frac{\hat{\alpha}_s^6}{N^6} + \ldots$$

- It is convenient to go from $(z, \mathbf{q}_T)$ to $(N, \mathbf{x}_T)$:
  1. Mellin convolutions over z turn into products: $\int \frac{dz}{z} \to \frac{1}{N}$
  2. Large logs map to poles at $N = 0$: $\alpha_s^{k+1} \ln^k \frac{1}{z} \to \frac{\alpha_s^{k+1}}{N^{k+1}}$
  3. All *collinear divergences* are in $\mathcal{C}$ in $\mathbf{x}_T$-space.

Expansion of $\hat{\sigma}_{\rm HEF}(\eta)$ in α_s **reproduces** $\hat{\sigma}_{\rm NLO}(\eta \gg 1)$ and predicts the $\hat{\sigma}_{\rm NNLO}(\eta \gg 1)$.

Matching with NLO

J.-Ph. Lansberg, M. Nefedov, M.A. Ozcelik, JHEP 05 (2022) 083

The HEF is valid in the **leading-power** in $M^2/\hat{s}$, so for $\hat{s} \sim M^2$: match with NLO CF

1. the *Inverse-Error Weighting Method* [Echevarria *et.al.*, 18']:

$$\hat{\sigma}(\eta) = w_{\rm CF}(\eta)\hat{\sigma}_{\rm CF}(\eta) + (1 - w_{\rm CF}(\eta))\hat{\sigma}_{\rm HEF}(\eta), \; w_{\rm CF}(\eta) = \frac{\Delta\hat{\sigma}_{\rm CF}^{-2}(\eta)}{\Delta\hat{\sigma}_{\rm CF}^{-2}(\eta) + \Delta\hat{\sigma}_{\rm HEF}^{-2}(\eta)}$$

$\Delta\hat{\sigma}_{\rm CF}(\eta)$ is due to **missing higher orders and large logarithms,**
$\Delta\hat{\sigma}_{\rm HEF}(\eta)$ is due to **missing power corrections in** $1/\eta$

2. the *Subtractive matching*: $\hat{\sigma}_{CF}(\eta) + \hat{\sigma}_{HEF}(\eta) - \alpha_s\tilde{\sigma}_1$, with
$\hat{\sigma}_{CF}(\eta \to \infty) = \hat{\sigma}_{HEF}(\eta \to 0) = \alpha_s\tilde{\sigma}_1$

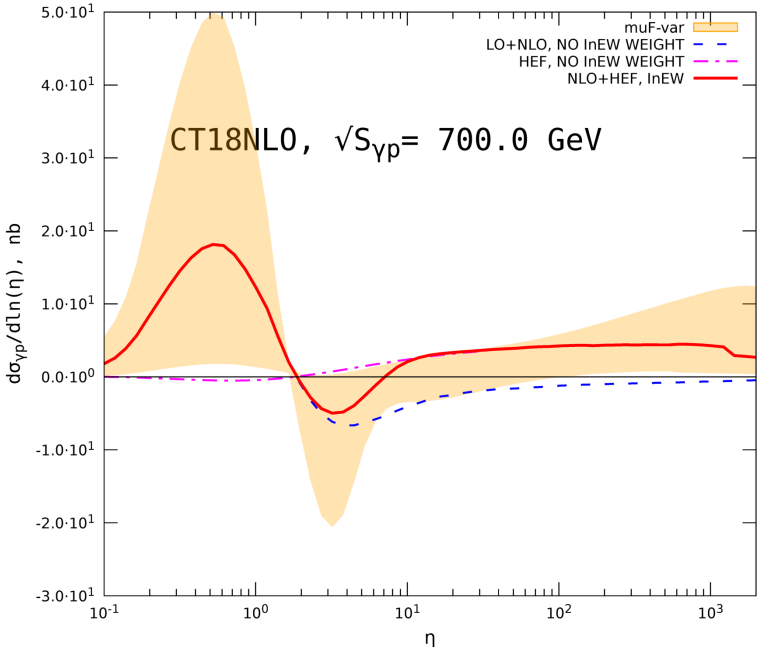

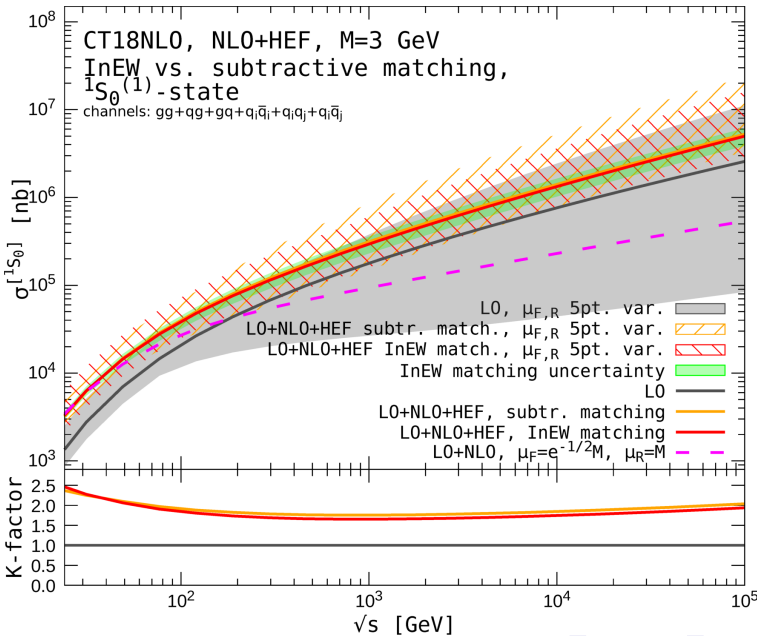

Matching with NLO for J/ψ inclusive photoproduction

J.-Ph. Lansberg, M. Nefedov, M.A. Ozcelik, JHEP 05 (2022) 083

Matched results for J/ψ photoproduction can be further improved by taking μ_F^2 and $\mu_R^2 \sim 25$ GeV^2 at high $\sqrt{s_{\gamma p}}$ for J/ψ

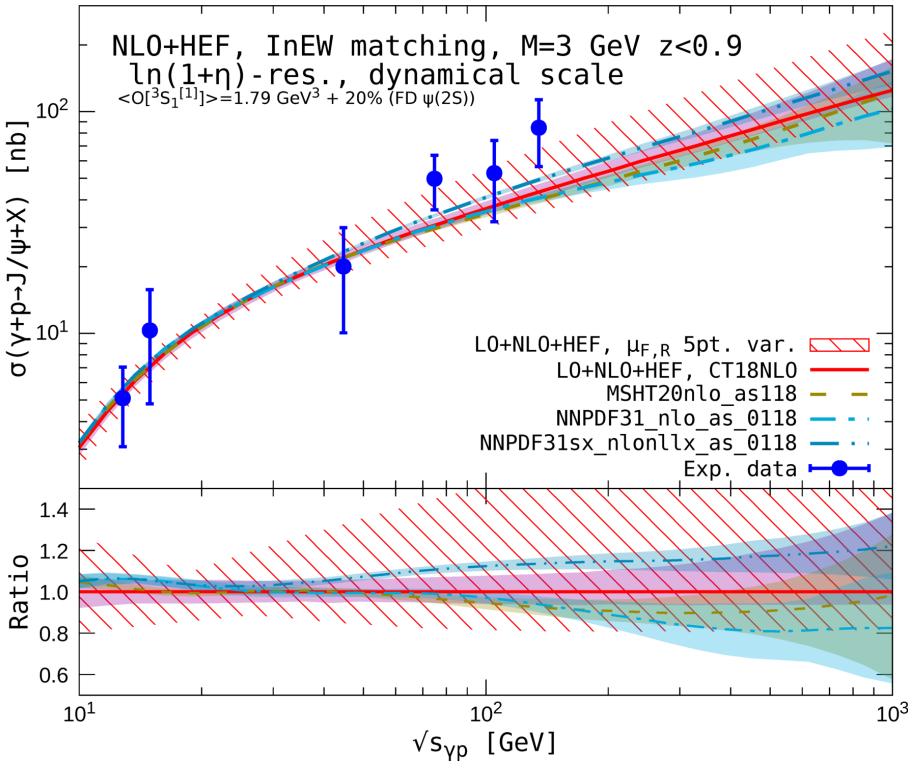

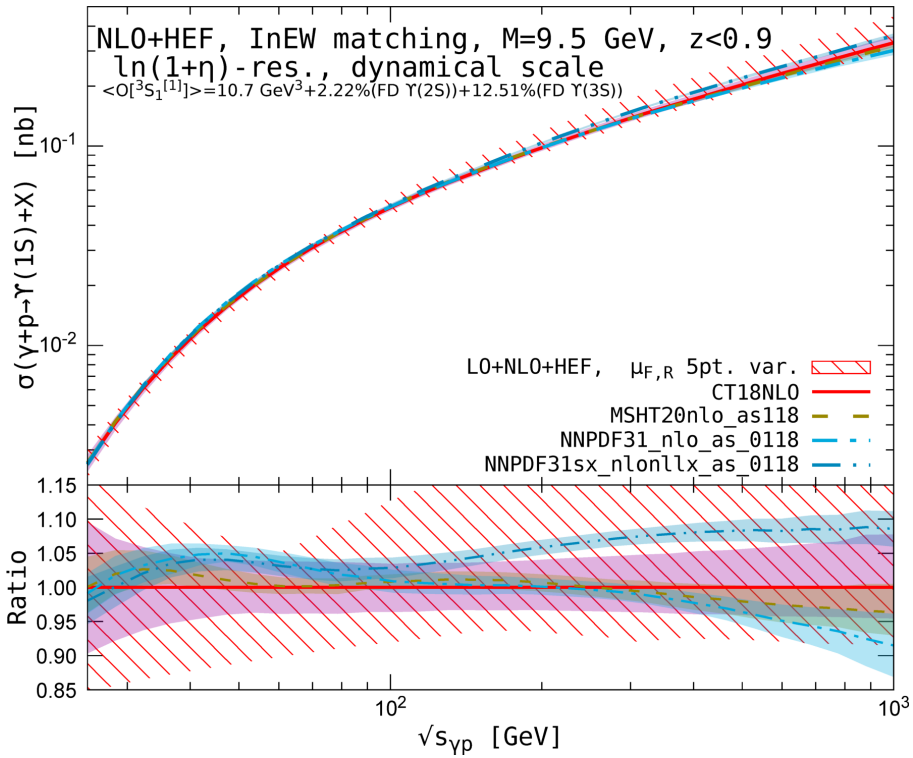

Part VII

Conclusions

Conclusions

- The CSM up to $\alpha\alpha_s^3$ reproduces photoproduction at HERA up to scale-uncertainty
- The estimations for the EIC can rely on CSM only
- NLO QCD corrections are important for P_T-integrated σ
- A specific μ_F choice can be employed to avoid a possible over subtraction of collinear divergences which lead to negative NLO σ values at large $\sqrt{s_{\gamma p}}$
- The perturbative instability of p_T-integrated quarkonium production cross sections at NLO comes from the region $\hat{s} \gg M^2$
- The problem can be solved via matching of NLO calculation at $\hat{s} \sim M^2$ and LLA HEF calculation at $\hat{s} \gg M^2$
- Loop correction matter and significant NNLO corrections (likely positive) are expected as well as a further reduction of the μ_R unc., esp. around 100 GeV
- This would likely allow one to better probe gluon PDFs at small-x and $\mu_F \sim M$.